Low-angle grain boundaries in $YBa_2Cu_3O_{7-\delta}$ with high critical current densities

R. Held, C. W. Schneider, and J. Mannhart
Experimentalphysik VI, Center for Electronic Correlations and Magnetism, Institute of Physics, Augsburg University, 86135 Augsburg, Germany

L. F. Allard, K. L. More, and A. Goyal
Materials Science and Technology Division, Oak Ridge National Laboratory, Oak Ridge, Tennessee 37831, USA
(Received 17 October 2008; revised manuscript received 27 November 2008; published 23 January 2009)

The grain-boundary network in high-T_c coated conductors consists of a large number of low-angle grain boundaries with many types of misorientation. Using the bicrystal technology we have measured the critical current densities of the relevant $YBa_2Cu_3O_{7-\delta}$ grain boundaries as a function of the grain-boundary angle. We find that in the low-angle regime [010]-tilt boundaries and [100]-twist boundaries reduce the critical current density much less than [001]-tilt boundaries. Transmission electron microscopy reveals a low defect density in the [010]-tilt boundaries and we find that CuO_2 planes cross these boundaries without interruption.

DOI: 10.1103/PhysRevB.79.014515 PACS number(s): 74.25.Sv, 74.25.Fy

I. INTRODUCTION

Alignment of the superconducting grains is the principle underlying the high-T_c coated conductor technologies, such as ion-beam-assisted deposition (IBAD) (Refs. 1 and 2) and rolling-assisted biaxially textured substrates (RABiTS),[3–6] and thus provides the key to fabricating competitive superconducting cables. The high-T_c coated conductors utilize polycrystalline superconducting films in which the grains are aligned along all major axes with a precision better than $\sim 8°$. The accurate alignment, most effectively in conjunction with large effective grain-boundary areas and doping of the grains,[7] is required because the grain-boundary critical current density J_c strongly decreases with increasing misalignment angle.[8,9]

While for $YBa_2Cu_3O_{7-\delta}$ (YBCO), the reduction in J_c has been explored in detail for [001]-tilt boundaries;[9] for other misorientations few data are available.[10] Samples with [100]-twist and [010]-tilt boundaries were explored by Dimos *et al.*,[8] who found that within the scatter of the data these boundaries had the same J_c values as [001]-tilt boundaries. Götz[11] observed the J_c of 8° and 16° [100]-twist boundaries to be less than the J_c of the corresponding [001]-tilt boundaries. Poppe and co-workers[12–14] reported that for angles between 21° and 28°, [010]-tilt boundaries with valley-type misorientation (Fig. 1) have a higher J_c than the corresponding [001]-tilt boundaries.

Coated conductors utilize grain boundaries with angles $\lesssim 8°$. To understand the requirements on the alignment of the grains, accurate data on the grain boundary J_c in this low-angle regime are therefore needed for all relevant grain misorientations. Here, we report such data and reveal that [010]-tilt and [100]-twist boundaries in $YBa_2Cu_3O_{7-\delta}$ are much less detrimental to J_c than previously known.

II. EXPERIMENTAL

The $YBa_2Cu_3O_{7-\delta}$ films were grown by pulsed laser deposition on nominally symmetric bicrystalline $SrTiO_3$ substrates[15] in 0.25 mbar of O_2 and at 750 °C. The substrates were TiO_2 terminated by etching in a buffered HF solution[16,17] with subsequent tempering at 950 °C for 10 h. The grain-boundary angles of the substrates were controlled

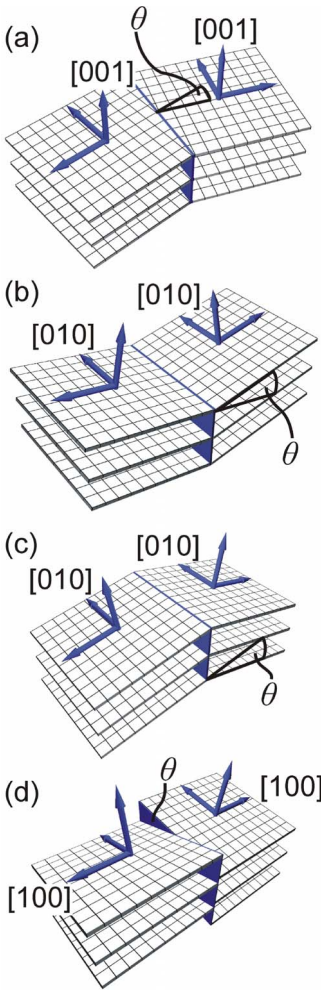

FIG. 1. (Color online) Illustrations of (a) [001]-tilt, (b) [010]-tilt valley-type, (c) [010]-tilt roof-type, and (d) [100]-twist grain boundaries in a cubic material.

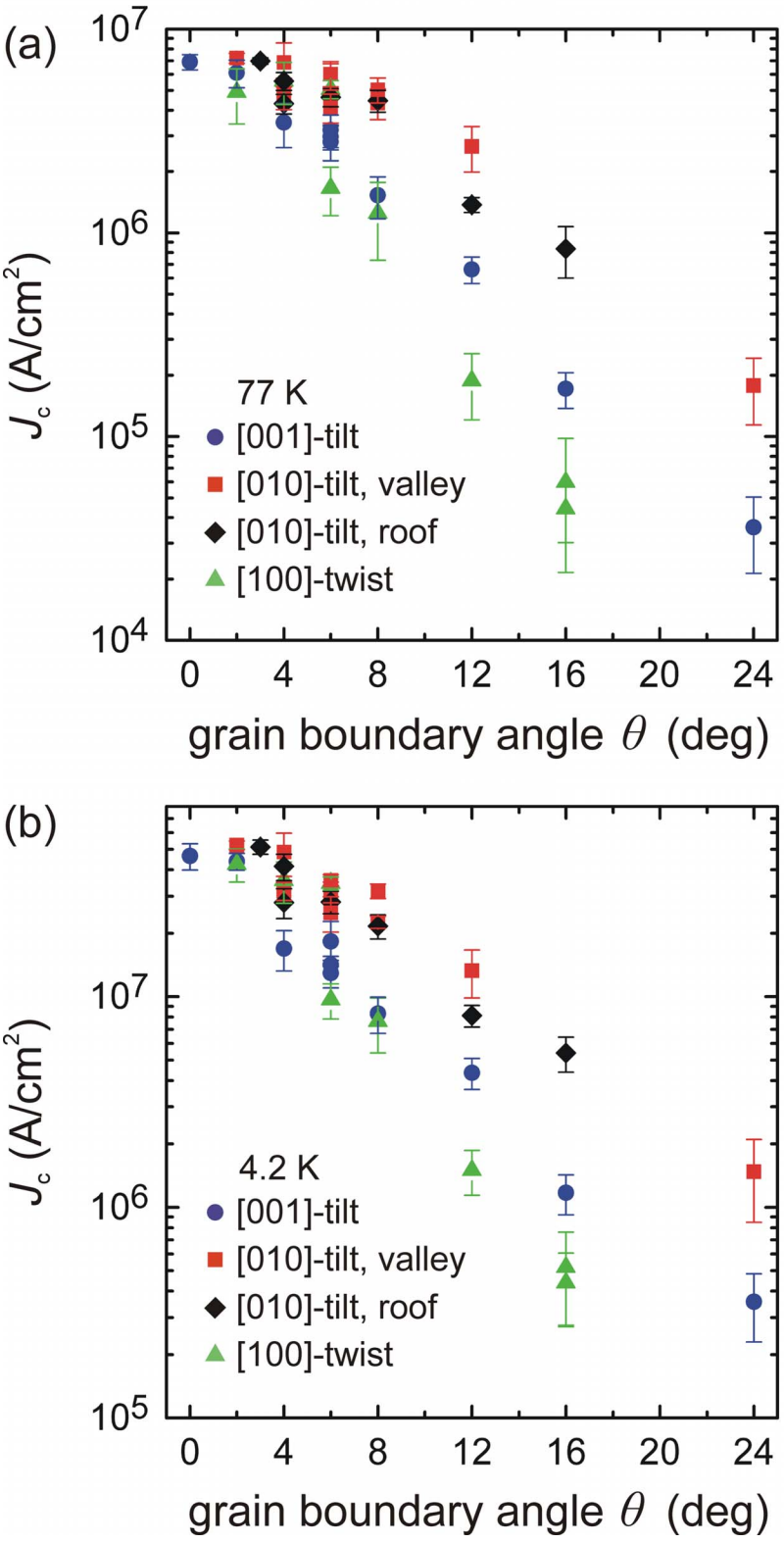

FIG. 2. (Color online) J_c of various types of bicrystalline grain boundaries in $YBa_2Cu_3O_{7-\delta}$ films measured at (a) 77 K and (b) 4.2 K as a function of misorientation angle. Please note that there are two data points for the 6° [100]-twist grain boundaries.

by x-ray diffraction to an accuracy of 0.2°. Undesired tilt and twist components are $<0.5°$ and the asymmetry component of all boundaries is $<1.0°$. By using photolithography and wet chemical etching the 100 ± 25 nm thick films were patterned into 3 to 5 μm wide and 20 μm long microbridges, aligned perpendicular to the grain boundary. Their critical currents I_c were derived from transport measurements using a 1 μV criterion, the J_c values were determined by dividing I_c by the cross-sectional area of the bridges as measured by scanning force microscopy (atomic force microscopy, AFM). The crystal structure of the $YBa_2Cu_3O_{7-\delta}$ films is of high quality as shown by x-ray diffraction. The grain boundaries were examined by AFM, transmission electron microscopy (TEM), and high-angle annular dark-field scanning transmis-

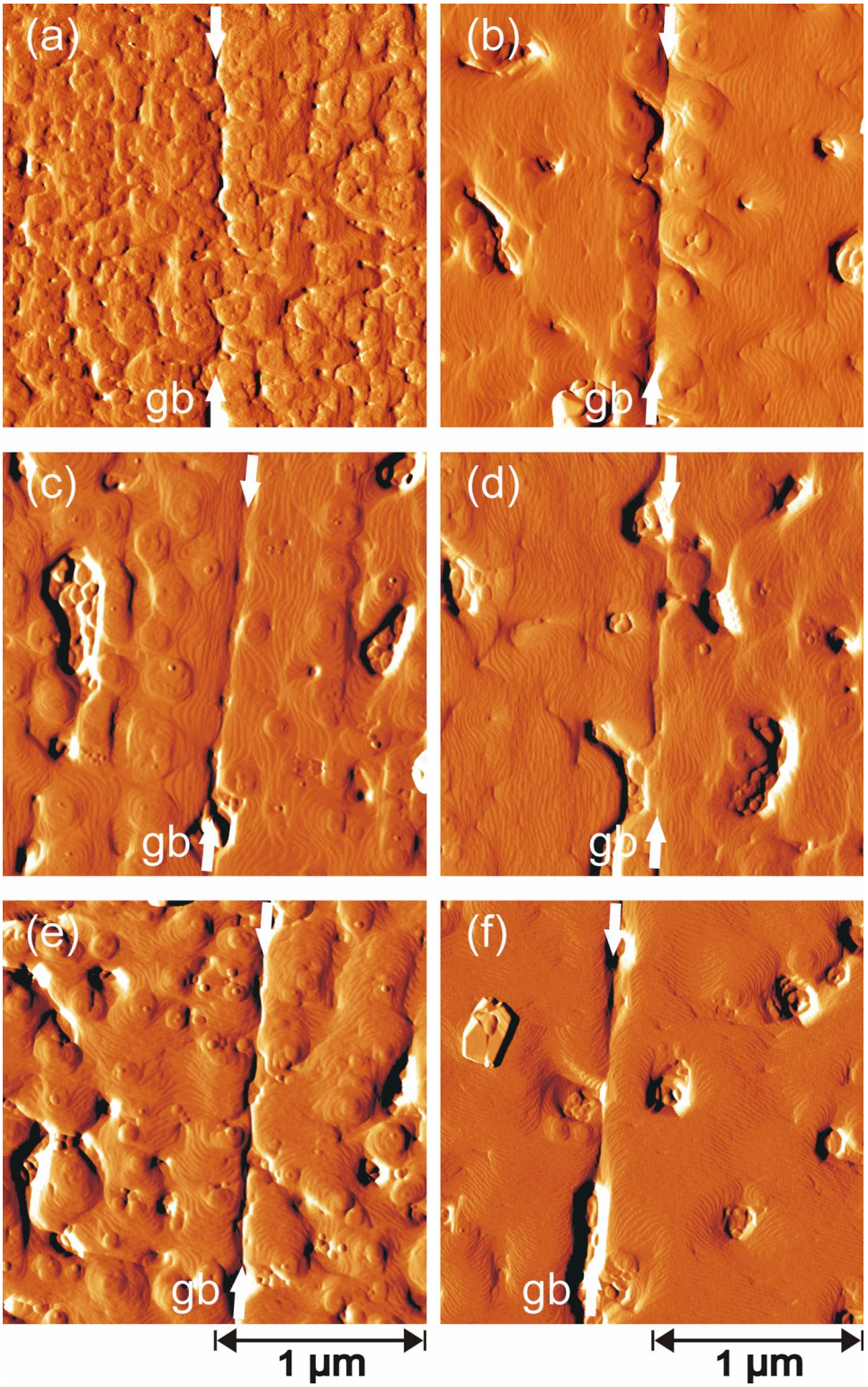

FIG. 3. (Color online) AFM micrographs of (a) $\theta=4°$ and (b) $\theta=8°$ [010]-tilt valley-type grain boundaries, (c) $\theta=4°$ and (d) $\theta=8°$ [010]-tilt roof-type grain boundaries, and (e) $\theta=4°$ and (f) $\theta=8°$ [100]-twist grain boundaries. The micrographs were taken in air using the tapping mode.

sion electron microscopy (HA-ADF STEM) of focused-ion-beam-milled (FIB-milled) cross sections taken from the boundary region.

III. RESULTS AND DISCUSSION

The grain-boundary critical current densities are plotted in Figs. 2(a) and 2(b). Each data point in the figure summarizes the measured J_c values of 6–8 bridges made on the same boundary. The [001]-tilt boundaries show the standard exponential reduction in J_c with increasing boundary angle which occurs for angles $\geq 2°$. The [010]-tilt and [100]-twist boundaries are characterized by a different angular dependence. Up to angles of 8° for [010]-tilt and 6° for [100]-twist boundaries, their J_c is reduced only by small amounts, remaining above 4×10^6 A/cm^2 and 5×10^6 A/cm^2 (77 K),

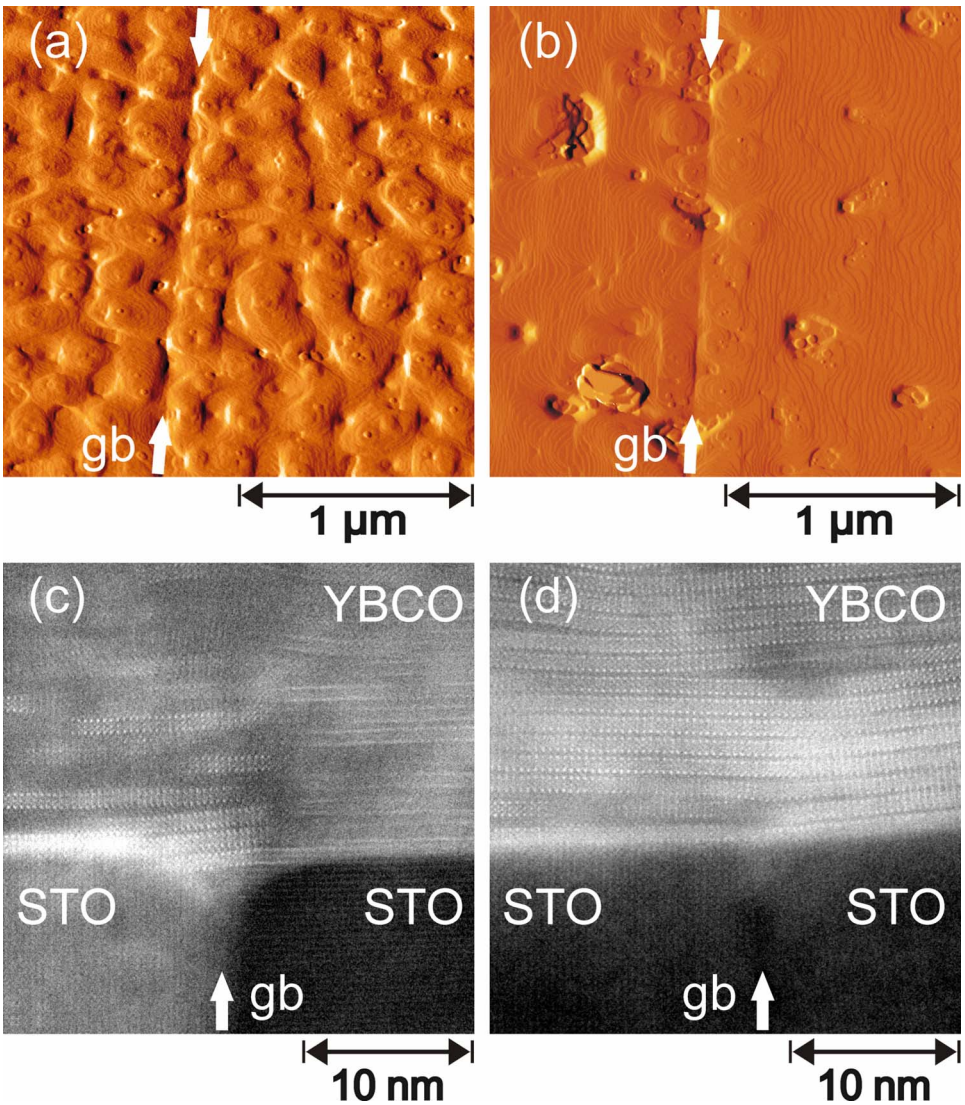

FIG. 4. (Color online) AFM micrographs of a (a) $\theta=6°$ [001]-tilt grain boundary and (b) a $\theta=6°$ [010]-tilt valley-type grain boundary. Cross-sectional HA-ADF STEM images of (c) a $\theta=6°$ [001]-tilt grain boundary and (d) a $\theta=6°$ [010]-tilt valley-type grain boundary.

respectively.[18] In the low-angle regime, the current densities of the [010]-tilt and [100]-twist boundaries thus differ significantly from the current densities of the [001]-tilt boundaries.

Here we have to ask whether this effect is associated with the vicinal cut[19] of the substrates containing out-of-plane boundaries. The vicinal cut influences the film growth and thereby the microstructure of the films. The AFM measurements presented in Figs. 3, 4(a), and 4(b) show that the growth mode of the YBCO films typically changes from an island- to a step-flow mode as the vicinal angle of the substrates increases. For samples with a vicinal angle of 2° both growth modes can be observed [see Figs. 3(a), 3(c), and 3(e)], suggesting that in this angular regime even small changes of the vicinal angle or of the growth parameters influence the growth mode. At larger vicinal angles [see Figs. 3(b), 3(d), 3(f), and 4(b)] only the step-flow growth mode was found, except for [010]-tilt valley-type grain boundaries, for which close to the boundaries island growth was detected for vicinal angles $\leq 6°$. This effect we attribute to the flat[20] regions which form at these bicrystal grain boundaries despite the vicinal cut of these substrates.

The microstructure of the grains influences the intragrain J_c. For vicinal cuts $\geq 2°$ (4.2 K) or $\geq 4°$ (77 K) we found the intragranular J_c of films grown on substrates with [010]-tilt boundaries to be smaller than the intragrain J_c of films without such a vicinal cut. For vicinal angles $\leq 6°$, the intragrain J_c of films grown on substrates with [100]-twist boundaries equals or may slightly exceed the J_c of films on substrates without a significant vicinal cut. For a vicinal angle of 8°, a small reduction in the grain J_c is observed for these substrates. These findings are consistent with the results of earlier investigations on the growth mode and the J_c anisotropy of YBCO films grown on vicinal substrates (see, e.g., Refs. 21–23).

While in the literature no consistent picture of a possible correlation between intragrain J_c and grain boundary J_c has been developed, the microstructure-induced changes in the intragrain J_c possibly alter the grain boundary J_c. Indeed, among samples with identical misorientation type and angle, the average grain boundary J_c was in most cases higher for samples exhibiting the higher intragrain J_c. Yet, in all cases in which this effect was found, it was small compared to the J_c reduction induced by the grain boundaries. Aside from this

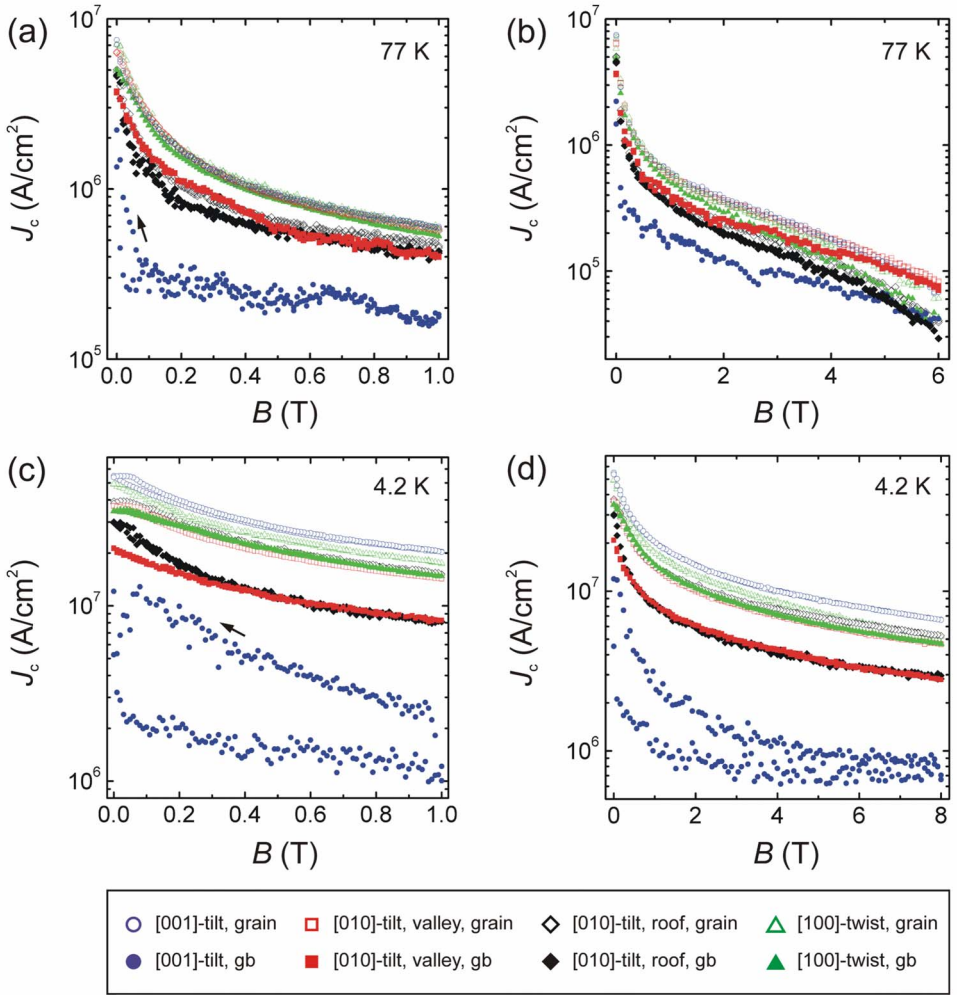

FIG. 5. (Color online) J_c of various types of $\theta=6°$ grain boundaries (gb) and of the corresponding grains in magnetic fields B applied in the boundary plane parallel to the substrate normal measured at (a) and (b) 77 K and (c) and (d) 4.2 K. The measured [100]-twist boundary is the one of the two 6° [100]-twist grain boundaries that has the higher J_c as shown in Fig. 2.

small correlation, we find that for the limited intragrain J_c variation of the samples investigated, the intragrain J_c merely sets an upper limit for the grain boundary J_c.

The differences of the transport properties of the grain-boundary types are also clearly observed in the magnetic field dependencies of J_c (Fig. 5). Remarkably, while the J_c [77 K, Figs. 5(a) and 5(b)] of 6° [001]-tilt boundaries is suppressed in an applied magnetic field of 0.1 T oriented perpendicular to the film surface by a factor of 8.9, such a field suppresses the J_c of the 6° [010]-tilt boundaries only by a factor of 2.3 or 3.2 for valley-type or roof-type boundaries, respectively. Likewise, the J_c of the 6° [001]-twist boundary is reduced by a factor of 2.1 only.

These results reveal that in coated conductors the out-of-plane misalignment is less detrimental to J_c than previously known. The requirements on the grain alignment along the corresponding directions are less demanding than considered in the literature.

At 4.2 K, the differences of the magnetic field dependencies of the grain boundary J_c values for grain boundaries with various types of misorientations are even more striking [Figs. 5(c) and 5(d)]. Whereas a magnetic field of 0.1 T suppresses the J_c of the 6° [001]-tilt boundary by a factor of 6.0, the J_c of the 6° [010]-tilt valley-type and roof-type boundaries is only reduced by factors of 1.2 and 1.4, respectively. Likewise, the J_c of the 6° [100]-twist boundary is suppressed by a factor of 1.1 only. Further, unlike at 77 K, the out-of-plane boundaries maintain their high J_c even in large magnetic fields [Fig. 5(d)]. The differences in the magnetic-field biased J_c of in-plane and out-of-plane boundaries at 4.2 K are thus found to be even larger than at 77 K.

How is it that the out-of-plane low-angle grain boundaries have such high critical current densities? The angular dependency of J_c is expected to differ between the various types of misorientations because of several reasons. J_c is reduced, for example, by the misalignment of the d-wave order-parameter lobes. While this reduction depends on the type of misorientation, it is not relevant in the low-angle range. At low-angle boundaries, however, the dislocations play a key role. The different types of boundaries result in different sets of dislocations and it is suggestive to associate the differences of J_c to the differences of the dislocation structure.

Therefore, to analyze the microstructure of the boundaries, grain boundaries of several $YBa_2Cu_3O_{7-\delta}$ films on 6° bicrystals of different misorientation types were investigated by AFM, TEM, and HA-ADF STEM imaging. Particular emphasis was given to the examination of the microstructures of [010]-tilt and [001]-tilt boundaries since they show the most significant difference in J_c. TEM specimens were prepared from several 6° bicrystals of both types and the entire grain boundaries in the samples were examined using TEM and HA-ADF STEM imaging.

While the AFM images [e.g., Figs. 3, 4(a), and 4(b)] show the expected microstructure at the $YBa_2Cu_3O_{7-\delta}$ surface, the HA-ADF STEM images from the cross-section FIB samples revealed surprising differences between the various types of boundaries. These are captured in the cuts through a 6° [001]-tilt boundary and through a 6° [010]-tilt valley-type boundary as shown in Figs. 4(c) and 4(d), respectively. The microstructure of the [001]-tilt boundary is characterized by the standard set of edge dislocations with [001]-oriented cores. This is the usual, well-known microstructure, which matches the well-known J_c of these samples. The microstructure of the [010]-tilt boundaries is different, however, and is characterized by a low density of stacking defects. As Fig. 4(d) shows, the misorientation of these boundaries is accommodated by bending of the $YBa_2Cu_3O_{7-\delta}$ unit-cell layers.

As a result, many of the YBCO unit-cell planes straddle the [010]-tilt boundaries without interruption, while the unit-cell planes are broken by [001]-tilt boundaries. The microstructural defects associated with this interruption are expected to suppress the superconducting order parameter, for example, by causing band bending due to the Coulomb interactions with unbalanced charges located at the defects.[24] The presence of uninterrupted $YBa_2Cu_3O_{7-\delta}$ unit-cell planes and the reduced density of dislocations therefore suggest themselves as explanation for the high J_c of the out-of-plane grain boundaries.

IV. SUMMARY AND CONCLUSIONS

In summary, we found that small-angle out-of-plane grain boundaries are much less detrimental to the J_c of YBCO films than in-plane grain boundaries. This effect is even more pronounced in applied magnetic fields. We attribute the high J_c of the out-of-plane boundaries to the special microstructure of these boundaries, characterized by uninterrupted unit-cell planes straddling the grain boundary. Our measurements yield the important result that for the production of coated conductors the requirements on the alignment of out-of plane grain boundaries can be relaxed.

ACKNOWLEDGMENTS

The work at the University of Augsburg was supported by the Bayerische Forschungsstiftung (Foroxid). Research at ORNL was supported partly by the U.S. Department of Energy, Office of Electricity Delivery and Energy Reliability-Superconductivity Program under Contract No. DE-AC05-00OR22725 with UT-Battelle, LLC managing contractor for Oak Ridge National Laboratory. Research was also supported in part by Oak Ridge National Laboratory's SHaRE User Facility, Division of Scientific User Facilities, Office of Basic Energy Science, U.S. Department of Energy. The authors gratefully acknowledge helpful discussions with S. Thiel and thank A. Herrnberger as well as K. Wiedenmann for their support.

[1] Y. Iijima, N. Tanabe, O. Kohno, and Y. Ikeno, Appl. Phys. Lett. **60**, 769 (1992).
[2] X. D. Wu, S. R. Foltyn, P. N. Arendt, W. R. Blumenthal, I. H. Campbell, J. D. Cotton, J. Y. Coulter, W. L. Hults, M. P. Maley, H. F. Safar, and J. L. Smith, Appl. Phys. Lett. **67**, 2397 (1995).
[3] A. Goyal, D. P. Norton, J. D. Budai, M. Paranthaman, E. D. Specht, D. M. Kroeger, D. K. Christen, Q. He, B. Saffian, F. A. List, D. F. Lee, P. M. Martin, C. E. Klabunde, E. Hartfield, and V. K. Sikka, Appl. Phys. Lett. **69**, 1795 (1996).
[4] D. P. Norton, A. Goyal, J. D. Budai, D. K. Christen, D. M. Kroeger, E. D. Specht, Q. He, B. Saffian, M. Paranthaman, C. E. Klabunde, D. F. Lee, B. C. Sales, and F. A. List, Science **274**, 755 (1996).
[5] A. Goyal, M. P. Paranthaman, and U. Schoop, MRS Bull. **29**, 552 (2004).
[6] A. Goyal, *Second Generation HTS Conductors* (Kluwer, Dordrecht, 2005).
[7] G. Hammerl, A. Herrnberger, A. Schmehl, A. Weber, K. Wiedenmann, C. W. Schneider, and J. Mannhart, Appl. Phys. Lett. **81**, 3209 (2002).
[8] D. Dimos, P. Chaudhari, and J. Mannhart, Phys. Rev. B **41**, 4038 (1990).
[9] See references listed in H. Hilgenkamp and J. Mannhart, Rev. Mod. Phys. **74**, 485 (2002).
[10] D. Larbalestier, A. Gurevich, D. M. Feldmann, and A. Polyanskii, Nature (London) **414**, 368 (2001).
[11] B. Götz, Ph.D. thesis, University of Augsburg, 2000.
[12] U. Poppe, Y. Y. Divin, M. I. Faley, J. S. Wu, C. L. Jia, P. Shadrin, and K. Urban, IEEE Trans. Appl. Supercond. **11**, 3768 (2001).
[13] Y. Y. Divin, U. Poppe, C. L. Jia, P. M. Shadrin, and K. Urban, Physica C **372–376**, 115 (2002).
[14] Y. Y. Divin, I. M. Kotelyanskii, P. M. Shadrin, C. L. Jia, U. Poppe, and K. Urban, in *Proceedings Applied Superconductivity (EUCAS)*, edited by A. Andreone, G. P. Pepe, R. Cristiano, and G. Masullo, IOP Conf. Proc. No. 181 (IOP, Bristol, 2003), p. 3112.
[15] Furuuchi Chemical Corporation, Fine Trading Division, Tokyo, Japan.
[16] M. Kawasaki, K. Takahashi, T. Maeda, R. Tsuchiya, M. Shinohara, O. Ishiyama, T. Yonezawa, M. Yoshimoto, and H. Koinuma, Science **266**, 1540 (1994).
[17] G. Koster, B. L. Kropman, G. J. H. M. Rijnders, D. H. A. Blank, and H. Rogalla, Appl. Phys. Lett. **73**, 2920 (1998).
[18] The critical current densities of the two 6° [100]-twist grain-boundary samples differ notably among the J_c of eight bridges on each sample. This suggests that the J_c of the boundaries is highly sensitive at this misorientation type and slight differences in misorientation angle and/or substrate grain-boundary microstructure and/or processing conditions may result in a significant change in J_c.
[19] Because the grain boundaries are symmetric, out-of-plane bicrystals with a boundary angle of θ have a vicinal angle of $\theta/2$.

[20] The density of the unit-cell steps does not exceed the density of unit-cell steps of substrates with a vicinal cut of 1°.
[21] T. Haage, J. Zegenhagen, J. Q. Li, H.-U. Habermeier, M. Cardona, Ch. Jooss, R. Warthmann, A. Forkl, and H. Kronmüller, Phys. Rev. B **56**, 8404 (1997).
[22] M. Djupmyr, G. Cristiani, H.-U. Habermeier, and J. Albrecht, Phys. Rev. B **72**, 220507(R) (2005).
[23] C. Cantoni, D. T. Verebelyi, E. D. Specht, J. Budai, and D. K. Christen, Phys. Rev. B **71**, 054509 (2005).
[24] H. Hilgenkamp and J. Mannhart, Appl. Phys. Lett. **73**, 265 (1998).